[American Journal of Science, Vol. 313, March, 2013, P. 242–266, DOI 10.2475/03.2013.03]

GEOCHEMISTRY OF THE ARVONIA FORMATION, CHOPAWAMSIC TERRANE, VIRGINIA: IMPLICATIONS FOR SOURCE AREA WEATHERING AND PROVENANCE

BRENT E. OWENS*, SCOTT D. SAMSON**, and SARAH E. KING***

ABSTRACT. The metasedimentary Arvonia Formation in the Piedmont Province of central Virginia ranges primarily from slates to garnet schists, which unconformably overly Middle Ordovician metavolcanic rocks of the Chopawamsic arc terrane. The formation has typically been interpreted as Late Ordovician based on poorly preserved fossils, perhaps having formed as a successor basin following accretion of the Chopawamsic arc to Laurentia. However, alternative interpretations have been proposed, including deposition outboard of Laurentia on Chopawamsic arc crust (that is, prior to accretion). Furthermore, the origin of the Chopawamsic arc as peri-Laurentian or peri-Gondwanan is an unresolved issue. We report whole-rock major and trace element compositions as well as Nd-isotopic compositions of the Arvonia Formation, and use these results to evaluate further its origin. Samples collected along the length of the outcrop belt show similar major element compositions, which are typical of shales. Chemical Index of Alteration values (68-89), corrected for K-metasomatism, indicate intermediate to extreme levels of source weathering. A majority of the samples show uniform rare-earth element (REE) patterns that are light REE-enriched with negative Eu-anomalies. A few samples display anomalous REE patterns, indicative of some disturbance of the light REE at approximately the time of deposition. A variety of trace element values or ratios indicate that Arvonia sediments are similar to shale composites (thus upper continental crust). Nd-isotopic compositions for eight samples are similar, with $\varepsilon_{Nd} = -5.6$ to -8.9 (400 Ma). Collectively, these results are consistent with derivation of Arvonia sediments from a single source or well-mixed sources of typical upper crustal composition. The isotopic data are compatible with a Laurentian provenance, however, they are equally compatible with a strictly Chopawamsic crustal source based on available Nd isotopic data.

Key words: Arvonia Formation, Chopawamsic Terrane, Piedmont Province, geochemistry, provenance

INTRODUCTION

The metasedimentary Arvonia Formation in the Piedmont Province of central Virginia (fig. 1) has attracted the attention of geologists for well over 175 years, since William Barton Rogers (the first state geologist of Virginia and founder of M.I.T.) commented in 1835 on the excellence of Arvonia slate as a roofing material (Rogers, 1884). In fact, quarrying of Arvonia slate has been ongoing for more than 250 years (Evans and Marr, 1988). In addition to its economic importance, the Arvonia Formation has figured prominently in the geologic story of this region because the slates contain "the richest fossil assemblage in the Piedmont terrane in the Southern Appalachians of the United States" (Kolata and Pavlides, 1986). Darton (1892) first identified crinoids in the slate, and additional fossils (bryozoa, trilobites, brachiopods) have been reported by other investigators since that time (Watson and Powell, 1911; Brown, 1969; Tillman, 1970; Kolata and Pavlides, 1986). Although the fossils are not well preserved, most paleontologists have considered them to be Middle to Upper Ordovician in age. Finally, the Arvonia Formation and correlative rocks (that is,

* Department of Geology, College of William and Mary, Williamsburg, Virginia 23187; beowen@wm.edu
** Department of Earth Sciences, Syracuse University, Syracuse, New York 13244
*** Department of Plant Sciences, University of California, Davis, California 95616

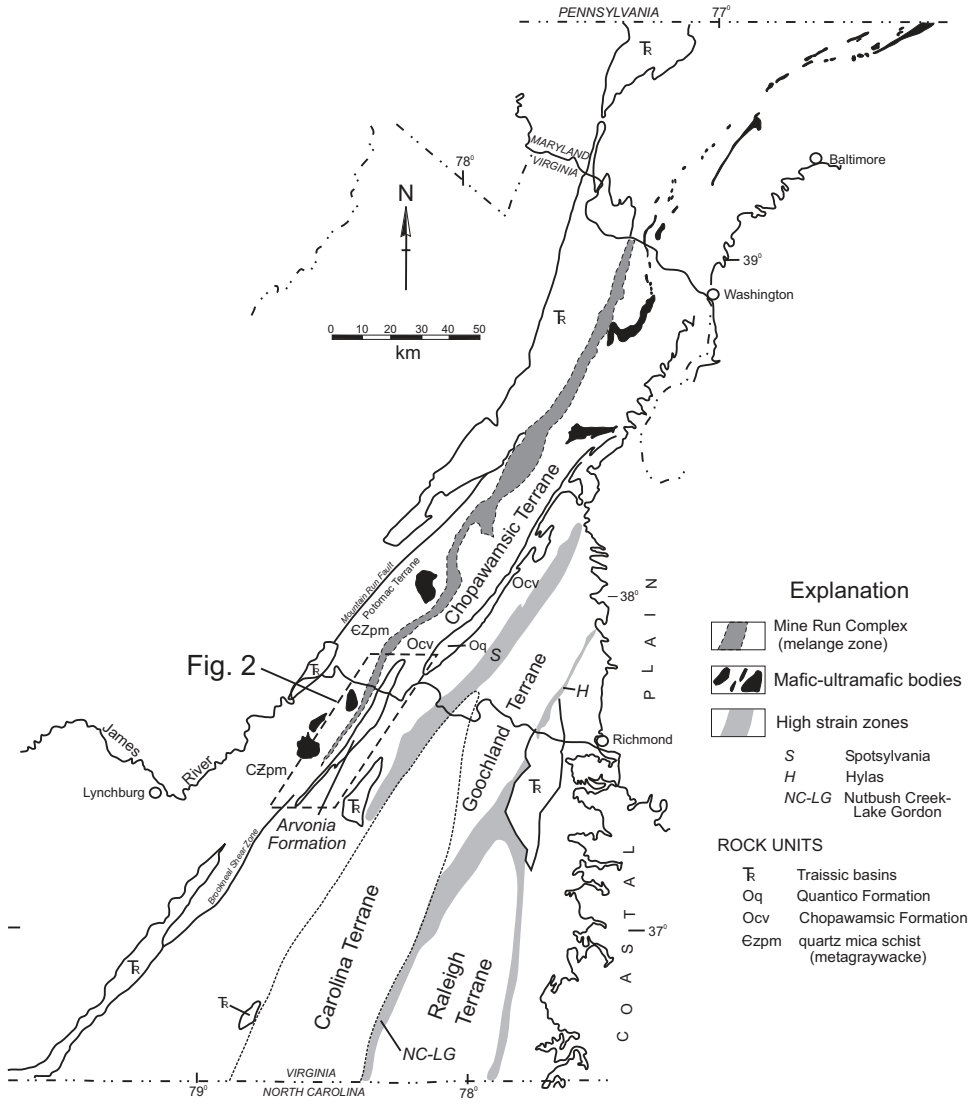

Fig. 1. Regional geologic map illustrating the location of the Arvonia Formation and various features of the Piedmont Province in Virginia. Simplified and modified from Brown (1986).

Quantico Formation) are the only Paleozoic sedimentary rocks in the Piedmont that post-date the Taconic orogeny (Glover and others, 1989).

The Arvonia Formation has at times been interpreted as a "successor" basin (for example, Dorsch, 1992) that formed following accretion of the Chopawamsic arc terrane (see below) to Laurentia. If true, the Arvonia sedimentary basin should have received substantial detritus from Laurentian sources. However, detrital zircon results reported by Bailey and others (2008) from basal quartzites in both the Arvonia and Quantico Formation (fig. 1) show a paucity of 1 to 2 Ga ages, a strong peak at 440 to 470 Ma, and a youngest age of 390 Ma. These results suggest: 1) that the Arvonia may be as young as Devonian; and 2) minimal to no contribution from Laurentian sources.

Similarly, Diecchio and Gottfried (2004) showed an interpretive sketch in which Arvonia sediments were deposited outboard of Laurentia on an unnamed microcontinent, that is, prior to accretion. Along these same lines, Hibbard and others (2007) suggested that the entire Chopawamsic belt (including the Arvonia Formation) might be of peri-Gondwanan rather than Laurentian affinity.

In this paper we use whole-rock major and trace element compositions as well as Nd-isotopic compositions to evaluate further the origin of the Arvonia Formation. Because shales (and in this case their metamorphosed equivalents) are efficient homogenizers of rocks in their source areas (for example, Taylor and McLennan, 1985; Garver and Scott, 1995; Patchett and others, 1999), their chemical compositions can provide valuable constraints on source area characteristics, including rock type, extent of weathering, and provenance (McLennan and others, 1993, 2003).

GEOLOGIC SETTING

As shown on figure 1, the Arvonia Formation occurs within the Chopawamsic Terrane of the central Piedmont Province of Virginia. Pavlides (1981) and Pavlides and others (1982) interpreted the Chopawamsic as a volcanic arc terrane on the basis of rock types and chemical compositions, and it is essentially equivalent to his central Virginia volcanic-plutonic belt (Pavlides, 1981). This belt makes up a major portion of what Hibbard and others (2007) referred to as the "Iapetan Realm" of the Appalachian orogen. The Iapetan Realm lies between the Laurentian Realm to the west, and the peri-Gondwanan realm to the east. The Iapetan Realm comprises various oceanic and magmatic arc rocks that were associated with the Iapetus Ocean.

Although long thought to be Cambrian, Coler and others (2000) reported U-Pb zircon ages on both volcanic and plutonic rocks from the Chopawamsic terrane that are middle Ordovician (~470-458 Ma). Additional Ordovician U-Pb zircon ages were later reported by Aleinikoff and others (2002), and most recently by Horton and others (2010). Coler and others (2000) also reported: 1) generally negative ε_{Nd} values for igneous rocks from the terrane; and 2) Mesoproterozoic xenocrystic zircons from metavolcanic rocks. Both of these results suggest that the terrane is composed of isotopically evolved crust. The terrane is bounded to the east by the Spotsylvania high strain zone (fig. 1), which separates it from the Goochland Terrane (Spears and others, 2004). Its western boundary is represented by the Brookneal shear zone, and also coincides approximately with the Mine Run Complex mélange zone (fig. 1). The Potomac Terrane lies west of this boundary.

The probable oldest rocks in the field area, of uncertain age, are the quartz-mica schists of the Potomac Terrane, west of the Mine Run Complex (figs. 1 and 2). These rocks have typically been interpreted as metagraywackes by previous investigators (for example, Brown, 1969). Evans (ms, 1984) referred to these rocks as the Hardware metagraywacke, but the unit currently has no formal stratigraphic name. The Diana Mills pluton is a mafic to ultramafic body with an age ~436 Ma (Wilson, ms, 2001) that occurs within metagraywackes west of the mélange zone.

The most widespread unit in the Chopawamsic Terrane is the Chopawamsic Formation (fig. 2). It consists primarily of a mixed suite of mafic and felsic metavolcanic rocks, as well as metasedimentary rocks, now represented by various amphibolites, felsic gneisses, and biotite gneisses. The formation also includes thin lenses (not shown on fig. 2) of other distinctive rock types including ferruginous quartzites (Peters and Owens, 2011) and metamorphosed ultramafic rocks (Owens and Uschner, 2001). Although kyanite quartzites at Willis and Woods Mts. (fig. 2) are included as part of the Arvonia Formation on the 1993 geologic map of Virginia, Owens and Pasek (2007) argued on mineralogical and geochemical grounds that these rocks represent hydrothermally altered volcanic rocks, now metamorphosed, and thus are part of the Chopawamsic Formation.

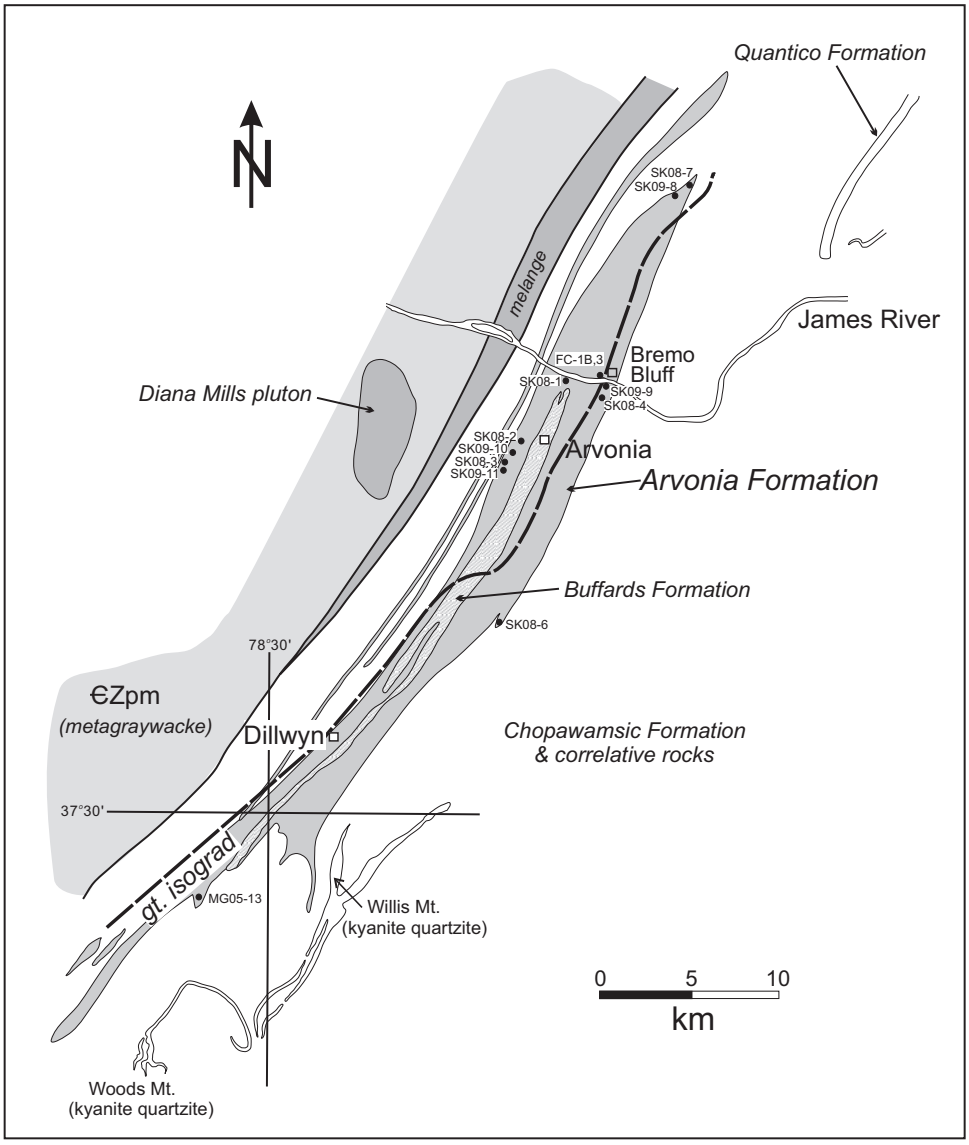

Fig. 2. Geologic sketch map of the Arvonia Formation field area, with sample locations indicated. The Bremo quartzite member occurs in a thin band near Bremo Bluff, but is not shown on this map. Map largely modified from Conley and Marr (1980), with additions based on Brown (1969) and the 1993 geologic map of Virginia (Virginia Division of Mineral Resources, 1993).

The Arvonia Formation forms a northeast-trending belt about 42 km in length in Buckingham and Fluvanna Counties, Virginia, with a maximum width of about 5 km. It lies unconformably on rocks of the Chopawamsic Formation (Stose and Stose, 1948). The formation includes the well-known commercial slates of this district, as well as higher-grade, more schistose and porphyroblastic equivalents. Brown (1969) mapped a garnet isograd that crosses the Arvonia in this area (fig. 2); lower-grade rocks occur to the northwest and higher-grade rocks to the southeast. The formation also includes

the Bremo Member, a prominent quartzite that makes up the bluffs along the James River near the town of Bremo Bluff (fig. 2). Most investigators have placed the Bremo member at the top of the Arvonia, but Brown (1969) argued that it occupies a more medial or even lower position, based on his interpretations regarding the Buffards Formation.

The Arvonia Formation occurs in a major synclinal structure, now overturned to the northwest, and the commercial slates are in the more northwesterly, lower-grade limb of this fold. Conley and Marr (1980), following Stose and Stose (1948), showed an intervening anticline, such that the structure is more complicated than a simple syncline. Evans and Marr (1988) also mapped a number of northeast-trending shear zones that cut the northeast limb of the syncline.

The Buffards Formation is a variably conglomeratic, quartz-mica phyllite and schist, whose outcrop belt lies in a band through the middle of the Arvonia Formation (fig. 2). The stratigraphic position of the Buffards Formation has been debated since Brown (1969) elevated the unit to formation status. Brown (1969) interpreted it to occupy the trough of the Arvonia syncline. Thus, in this interpretation, the Buffards lies above the Arvonia. In contrast, Stose and Stose (1948) correlated Buffards conglomeratic rocks with other conglomerates at the base of the Arvonia, and most other investigators have favored this interpretation (Conley and Marr, 1980; Evans and Marr, 1988).

METHODS

Portions of each sample were crushed to a fine powder using procedures similar to those described by Dymek and Owens (2001). Most samples were analyzed for major and trace elements, including the rare earth elements, by inductively coupled plasma (ICP) and ICP-MS (mass spectrometry) methods by Activation Laboratories, Ltd., Ontario. The method involves a lithium metaborate/tetraborate fusion of the sample prior to digestion to ensure dissolution of resistate phases. Values for some trace elements (As, Mo, Ag, In, Bi) determined by ICP-MS that are below the limits of detection are not reported. The major elements for one sample (FC-1B, Bremo quartzite) were determined by X-ray fluorescence methods (XRF) at Washington University in St. Louis, using procedures described by Couture and others (1993). Selected trace elements (Sn, Nb, Zr, Y, Sr, Rb, Pb, Ga, Zn, Ni, V, Cr, Ba, Co) were also determined in two samples (FC-1B, FC-3) by XRF using procedures described by Couture and Dymek (1996). The overall agreement between XRF and ICP-MS methods for elements that were analyzed by both techniques is excellent, but only the values determined by Activation Laboratories are reported here.

A subset of samples was also analyzed for Nd-isotopic compositions. Analytical protocols for whole-rock dissolution, chemical separation of Sm and Nd, and mass spectrometry follow those described in Samson and others (1995). The only exception is that the ^{149}Sm-^{150}Nd tracer "spike" solution was added to samples prior to high temperature HF dissolution.

SAMPLING AND PETROGRAPHY

We collected 13 hand samples of the Arvonia Formation for whole-rock analysis, including one sample of Bremo quartzite. Our goals in sampling were to collect from along the length of the formation and to include samples of both slate and schist. All samples to the east of the garnet isograd are schists, but some rocks west of the isograd are also schistose. Sample locations are shown on figure 2. We found that rocks to the south are pervasively streaked with quartz veins, so fewer samples come from that area. Slate samples were collected from two active quarries, several small abandoned pits, and outcrop. Schist samples come mostly from outcrop, but one (SK09-9) was obtained

from a railroad cut on the south side of the James River. The Bremo quartzite sample (FC-1B) was collected at the base of a high bluff on the north side of the James River.

Slates are fine-grained, dark gray, and variably porphyroblastic. Dominant minerals include muscovite and quartz, with lesser amounts of chlorite, plagioclase, opaques, and carbonate in some cases. Porphyroblasts locally include biotite or pyrite. Schists east of the garnet isograd are lighter gray, and typically contain both biotite and garnet porphyroblasts. A thin section from sample MG05-13 contains a single grain of staurolite, suggesting the presence of an ill-defined staurolite isograd across the map area. Trace amounts of tourmaline and zircon occur in both rock types. In addition to quartz, the Bremo quartzite sample contains >10 percent chlorite, and trace amounts of garnet.

WHOLE-ROCK COMPOSITIONS

Whole-rock major and trace element compositions are listed in table 1. Nd-isotopic compositions of eight selected samples are listed in table 2.

Classification

Herron (1988) provided a geochemical classification for clastic sedimentary rocks based on the ratios SiO_2/Al_20_3 and Fe_2O_3/K_2O (with all Fe as Fe_2O_3). Although diagenesis and metamorphism may have perturbed the major element compositions, most Arvonia samples plot in the field for shale on Herron's diagram (fig. 3), consistent with the inferred protolith. Two fall in the wacke field, and the Bremo quartzite sample (FC-1B) plots in the Fe-sand field.

Major Elements

On figure 4, Arvonia slate and schist compositions are compared to the average post-Archean Australian shale (PAAS) of Taylor and McLennan (1985). Major element compositions are similar to PAAS (fig. 4), apart from CaO, which is clearly depleted in all samples. Sample SK09-8 is depleted in most oxides relative to PAAS, but this sample has higher weight percent SiO_2 than the rest. Thus, this depletion reflects dilution by quartz.

The major element compositions of slates and schists are illustrated on a series of Al_20_3 variation diagrams on figure 5. Slates and schists are distinguished on these plots, and for most oxides there are no systematic differences between them. A subset of four slates has slightly higher amounts of MgO, but otherwise the compositions of the two rock types show considerable overlap and scatter. Crude negative and positive arrays for SiO_2 (r^2=0.44) and K_2O (r^2=0.41), respectively, with Al_2O_3 may reflect variable amounts of quartz and clay in the original muds (although the correlation with SiO_2 may simply reflect closure). Because slate and schist compositions are similar, they are not distinguished on subsequent diagrams.

Trace Elements

Concentrations of selected trace elements are compared to PAAS on figure 6. Compositions are for the most part similar to PAAS, but Sr is clearly depleted. The consistent depletions in CaO and Sr could reflect a source area that was poorer in plagioclase than that for PAAS, or one that had undergone a higher degree of weathering. Nickel is also depleted in all but one sample compared to PAAS, further suggesting a different average source composition. Consistent with its major element composition, sample SK09-8 is depleted in most elements relative to PAAS, particularly the ferromagnesian elements (Ni, Sc, Cr, V, Zn), Zr and Pb.

Chondrite-normalized concentrations of the rare earth elements (REE) are illustrated on figure 7. Eight samples have similar patterns (fig. 7A) that are light REE-enriched (La_N/Yb_N = 7.2-10.2), with relatively flat heavy REE slopes (Gd_N/Yb_N =

TABLE 1

Whole-rock major and trace element compositions of Arvonia Formation samples (major elements in wt.%; trace elements in ppm)

Sample	SK08-1	SK08-2	SK08-3	SK08-4	SK08-6	SK08-7	SK09-8	SK09-9	SK09-10	SK09-11	MG05-13	FC-3	FC-1B
Rock type	slate	slate	slate	schist	schist	slate	schist	schist	slate	slate	schist	schist	quartzite
SiO_2	64.95	60.61	64.02	65.86	64.97	61.76	71.15	64.56	62.47	63.61	58.36	67.71	92.14
TiO_2	0.98	1.01	1.04	1.03	1.01	0.94	0.45	0.99	0.99	0.97	1.06	1.04	0.15
Al_2O_3	14.02	16.23	16.92	16.44	17.09	18.03	15.59	16.99	16.61	16.58	20.54	15.42	2.52
Fe_2O_3(T)	7.65	8.09	6.99	6.40	6.65	7.42	3.85	6.63	8.18	7.60	8.34	4.96	3.73
MnO	0.11	0.16	0.03	0.05	0.06	0.04	0.04	0.05	0.09	0.07	0.05	0.03	0.21
MgO	2.25	2.78	1.64	1.58	1.53	1.59	1.22	1.68	2.58	2.67	1.74	1.57	0.36
CaO	0.73	0.80	0.12	0.38	0.60	0.15	0.03	0.59	0.30	0.04	0.22	0.21	0.06
Na_2O	1.98	1.73	1.34	1.15	1.14	0.59	0.25	1.31	1.47	1.48	1.21	1.17	0.29
K_2O	2.56	3.70	3.40	3.35	3.70	3.80	3.86	3.70	3.55	3.61	4.11	3.93	0.19
P_2O_5	0.19	0.19	0.15	0.15	0.10	0.08	0.11	0.14	0.24	0.14	0.13	0.08	0.04
LOI	3.25	4.10	3.39	2.86	2.22	3.96	3.50	2.88	3.70	3.72	3.36	2.81	0.65
Total	98.67	99.40	99.04	99.25	99.07	98.36	100.05	99.52	100.18	100.49	99.12	98.93	100.34
CIA	67	67	74	74	72	78	77	71	73	72	76	71	79
*CIA**	*68*	*70*	*80*	*79*	*78*	*85*	*89*	*78*	*79*	*79*	*82*	*79*	na
Sc	15	19	19	18	19	19	8	18	18	19	22	17	nd
V	136	162	163	146	166	182	64	155	168	175	187	125	15
Cr	60	80	80	100	70	80	<20	70	80	80	90	70	<20
Co	18	19	9	12	10	9	7	13	17	7	11	2	7
Ni	<20	20	70	<20	<20	30	<20	<20	<20	<20	<20	<20	<20
Cu	30	50	<10	<10	10	20	<10	20	60	50	10	<10	20
Zn	100	140	110	110	120	130	50	90	100	90	150	100	<30
Ga	18	23	22	21	22	25	17	22	22	23	27	20	4
Ge	2	2	2	2	2	2	1.9	2.5	3.2	2.6	2	2	1.2
Rb	102	154	152	152	150	194	123	160	139	135	162	172	10
Sr	102	112	83	81	126	88	104	95	93	81	99	61	7
Y	30	37	34	36	32	32	21.9	23.5	38.9	27.3	42	29	13.5
Zr	240	154	211	255	227	180	128	260	168	168	167	296	94
Nb	14	16	18	18	17	17	11.6	16.5	16.1	13.6	17	19	3.4
Ba	397	506	627	604	612	670	794	640	445	1198	870	696	34

Table 1
(continued)

Sample	SK08-1	SK08-2	SK08-3	SK08-4	SK08-6	SK08-7	SK09-8	SK09-9	SK09-10	SK09-11	MG05-13	FC-3	FC-1B
Rock type	slate	slate	slate	schist	schist	slate	schist	schist	slate	slate	schist	schist	quartzite
Cs	4.4	7.1	6.6	4.4	6.2	9	3	5	6.2	5.3	6	7	0.7
Sn	2	3	3	3	3	4	1	4	4	3	4	3	<1
Sb	<0.5	1.3	<0.5	<0.5	<0.5	<0.5	<0.2	<0.2	1.8	<0.2	<0.5	<0.5	<0.2
La	39.2	45.8	45.9	56.2	49.7	18.4	170	11	55.8	32.1	49.8	4.3	11.5
Ce	80.7	94.4	95.5	108	102	34.9	120	27.4	99.8	67.5	102	7.2	28.3
Pr	8.53	12.1	12.2	11.3	10.4	4.91	31.6	3.13	12.2	7.18	12.8	0.98	3.01
Nd	31.2	40.5	39.4	41	36.9	17.4	117	11.8	50.2	27.6	42.2	4.1	12.4
Sm	6.9	8.2	8	8.9	7.9	3.7	18.3	2.4	10.1	5.96	8.3	1.1	3.36
Eu	1.57	1.72	1.7	1.81	1.61	0.84	4.13	0.53	1.96	1.31	1.66	0.38	0.702
Gd	5.5	7.4	6.8	6.4	4.6	3.6	10.9	1.98	8.87	5.45	7.3	2.3	3.43
Tb	0.9	1.1	1	1.1	0.9	0.7	1.54	0.47	1.4	0.98	1.2	0.6	0.5
Dy	5.5	6.5	6.1	6.6	6	5	7.01	3.57	7.87	5.46	7.1	4.8	2.57
Ho	1.1	1.3	1.3	1.3	1.3	1.1	1.06	0.89	1.57	1.11	1.5	1.2	0.38
Er	3.3	4.1	4.1	4	3.9	3.5	2.5	2.79	4.28	3.1	4.7	4	1.22
Tm	0.48	0.62	0.61	0.59	0.58	0.52	0.339	0.481	0.650	0.468	0.71	0.6	0.174
Yb	3	3.8	3.8	3.7	3.6	3.3	2.02	3.35	4.05	3.01	4.3	3.8	1.13
Lu	0.45	0.56	0.57	0.55	0.55	0.5	0.275	0.501	0.535	0.417	0.64	0.6	0.188
Hf	6.4	5.3	7	6.9	6.4	5.5	3.4	6.6	4.6	4.5	5.3	10.2	2.4
Ta	1.3	1.3	1.4	1.7	1.7	1.3	1.31	1.43	1.24	1.21	1.4	1.6	0.28
W	1	<1	1	1	1	1	8.5	3.1	1.9	2.4	<1	1	<0.5
Tl	0.8	2.3	1.9	1.2	1.6	2.3	0.56	0.62	0.59	0.56	1.6	2.3	<0.05
Pb	10	23	17	21	24	27	9	13	14	13	16	22	<5
Th	10.7	13	13.2	13.4	13.9	13.8	15	12.3	14.2	13.5	14	12.2	3.22
U	3.1	4	3.4	3.2	3.5	3.3	5.57	3.60	3.86	4.47	3.4	3.7	0.95
La_N/Yb_N	8.81	8.13	8.14	10.24	9.31	3.76	56.7	2.21	9.29	7.19	7.81	0.76	6.86
Gd_N/Yb_N	1.48	1.57	1.44	1.40	1.03	0.88	4.35	0.48	1.77	1.46	1.37	0.48	2.45
Eu/Eu*	0.78	0.68	0.70	0.73	0.82	0.70	0.89	0.74	0.63	0.70	0.65	0.73	0.63

* Italicized CIA values are corrected for K-metasomatism (see text for discussion).
na = not applicable.
nd = not determined.

TABLE 2

Nd isotopic compositions of Arvonia Formation samples

Sample no.	Field no.	$^{147}Sm/^{144}Nd$	$^{143}Nd/^{144}Nd$[a]	$f_{Sm/Nd}$[b]	$\varepsilon_{Nd}(0)$[c]	$\varepsilon_{Nd}(T)$[d]	T_{DM1}[e] (Ga)	T_{DM2}[f] (Ga)
1	SK08-1	0.1327	0.512028 ± 5	-0.3250	-11.90	-8.64	1.91	
2	SK08-4	0.1302	0.512079 ± 3	-0.3377	-10.90	-7.51	1.77	
3	SK08-7	0.1276	0.512075 ± 5	-0.3510	-10.98	-7.46	1.73	
4	SK09-9	0.1229	0.512083 ± 10	-0.3749	-10.83	-7.07	1.64	
5	SK09-10	0.1220	0.511989 ± 2	-0.3795	-12.65	-8.85	1.74	
6	MG05-13	0.1189	0.512083 ± 6	-0.3952	-10.83	-6.86	1.57	
7	FC-3	0.1662	0.512250 ± 13	-0.1546	-7.57	-6.02	2.45	1.55
8	FC-1B	0.1626	0.512261 ± 12	-0.1729	-7.35	-5.62	2.33	1.51

[a] Measured ratio, corrected for spike and normalized to $^{146}Nd/^{144}Nd = 0.7219$. Uncertainties are $+2\sigma$ and refer to least significant digit.
[b] $f_{Sm/Nd} = [(^{147}Sm/^{144}Nd)_{sample}/0.1966] - 1$.
[c] $\varepsilon_{Nd}(0)$ indicates present-day epsilon value; present-day Bulk Earth values: $^{143}Nd/^{144}Nd = 0.512638$; $^{147}Sm/^{144}Nd = 0.1966$.
[d] $\varepsilon_{Nd}(T)$ calculated for a depositional age of 400 Ma.
[e] Depleted mantle model age following model of DePaolo (1981).
[f] Secondary model age using $(^{147}Sm/^{144}Nd)_{sample}$ to 400 Ma then using $(^{147}Sm/^{144}Nd)_{shale\ mean}$ (that is, 0.1257) until intersection with depleted mantle model of DePaolo (1981).

1.03-1.77), and negative Eu-anomalies (Eu/Eu* = 0.63-0.82). The pattern shapes of these samples are much like that of PAAS (fig. 7B) but overall concentrations of most are slightly enriched. Two samples (SK08-7, SK09-9) have lower concentrations of the light and middle REE (figs. 7A and 7B), less fractionated patterns (La_N/Yb_N = 2.2, 3.8), and Gd_N/Yb_N values <1 (0.88, 0.48).

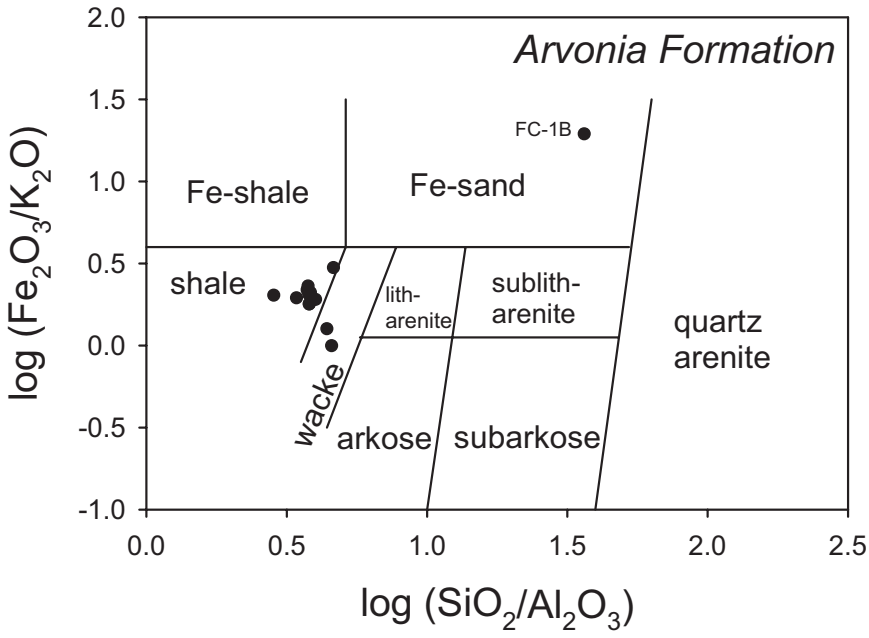

Fig. 3. Geochemical classification diagram of Herron (1988) for clastic sedimentary rocks. Arvonia samples plot primarily in the shale field.

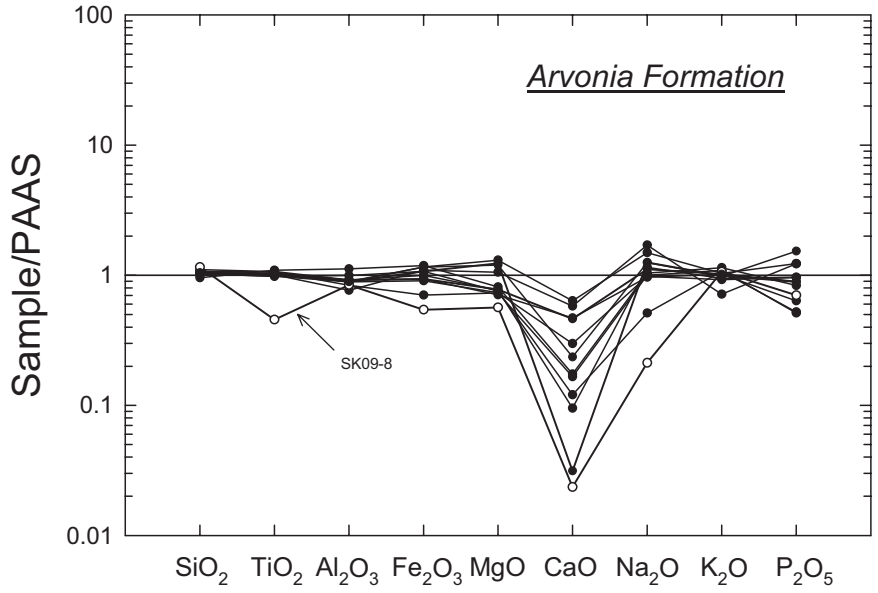

Fig. 4. Major element compositions of Arvonia samples normalized to Post-Archean Australian Shale (PAAS). Normalizing values from Taylor and McLennan (1985).

Two samples (SK09-8, FC-3) have anomalous patterns (fig. 7C). Sample FC-3 is extremely depleted in the light REE, such that LREE < HREE. In contrast, sample SK09-8 has a highly fractionated pattern ($La_N/Yb_N = 56.7$), is greatly enriched in the LREE ($La_N = 548$), and shows a negative Ce-anomaly. The single sample of Bremo quartzite (FC-1B) has concentrations of the LREE that are similar to samples SK08-7 and SK09-9, but is depleted in the HREE.

Nd-Isotopic Compositions

Measured $^{143}Nd/^{144}Nd$ ratios range from 0.512028 to 0.512261, leading to ε_{Nd} (400 Ma) values with a fairly narrow range from −5.8 to −8.9 (average = −7.3). We consider 400 Ma to be a reasonable estimate for the age of deposition based on the detrital zircon results reported by Bailey and others (2008). Values calculated for a slightly older depositional age of 450 Ma, the maximum possible depositional age based on the crystallization age of volcanic rocks in the underlying Chopawamsic Formation, are different by less than 0.5 ε_{Nd} unit. The results for six samples with similar $^{147}Sm/^{144}Nd$ ratios (0.12-0.13) yield depleted mantle model ages (T_{DM}) that range from 1.57 to 1.91 Ga. The anomalous sample FC-3 and the quartzite FC-1B have high enough $^{147}Sm/^{144}$ Nd ratios (0.166 and 0.163, respectively) that unrealistically old model ages are calculated (2.45 and 2.33 Ga). It is possible that for these two samples their $^{147}Sm/^{144}Nd$ ratios were modified by diagenetic alteration shortly after deposition. If it is assumed that both samples had $^{147}Sm/^{144}Nd$ similar to the average value of the other samples (that is, 0.1257) then a secondary, or two-stage, model age (T_{DM2}) can be calculated. This is done by determining $^{143}Nd/^{144}Nd$ at 400 Ma using measured ratios then continuing to project $^{143}Nd/^{144}Nd$ back through time using the mean $^{147}Sm/^{144}Nd$ (0.1257) of the other sedimentary rocks until intersection with the depleted mantle occurs. For schist sample FC-3 the T_{DM2} age is 1.55 Ga and for quartzite FC-1B it is 1.51 Ga. The Nd-isotopic results are illustrated on an ε_{Nd} versus time plot on figure 8.

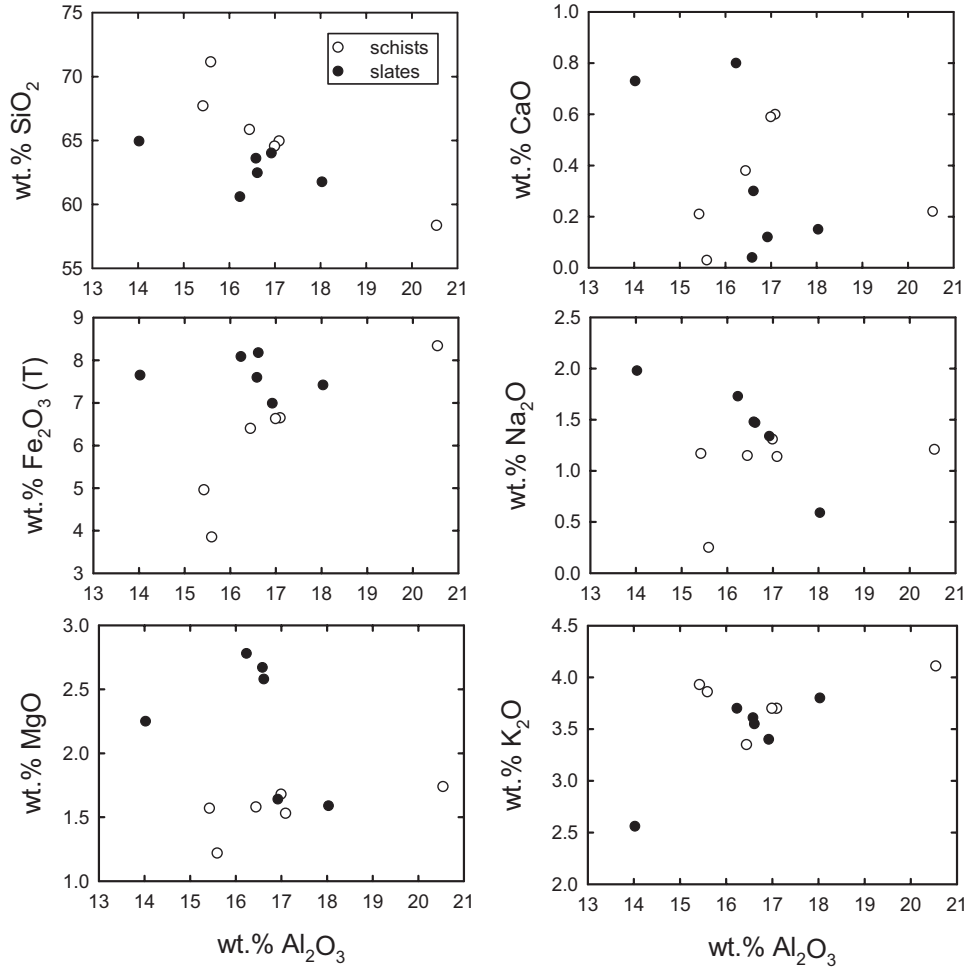

Fig. 5. Major element, Al_2O_3-variation diagrams for Arvonia Formation schists and slates.

DISCUSSION

The chemical composition of a given clastic sedimentary rock is a cumulative and complex result of several factors, including: 1) the nature of the source rock; 2) extent of weathering of the source; 3) sedimentary processes such as sorting; and 4) possible element mobility during diagenesis (Sawyer, 1986; McLennan and others, 1993; McLennan and others, 2003). In the following sections, we use our geochemical results to gain insights into those factors that led to the compositions of Arvonia Formation sediments.

Source Area Weathering

The principal effect of progressive chemical weathering is to increase the clay content of the weathered material, as well as to increase the abundance of weathering-resistant minerals such as quartz and zircon. The breakdown of plagioclase, in particular, typically leads to an increase in clay content, and loss of mobile Ca^{2+} and Na^{1+} cations (Nesbitt and Young, 1982). The Chemical Index of Alteration (CIA) of

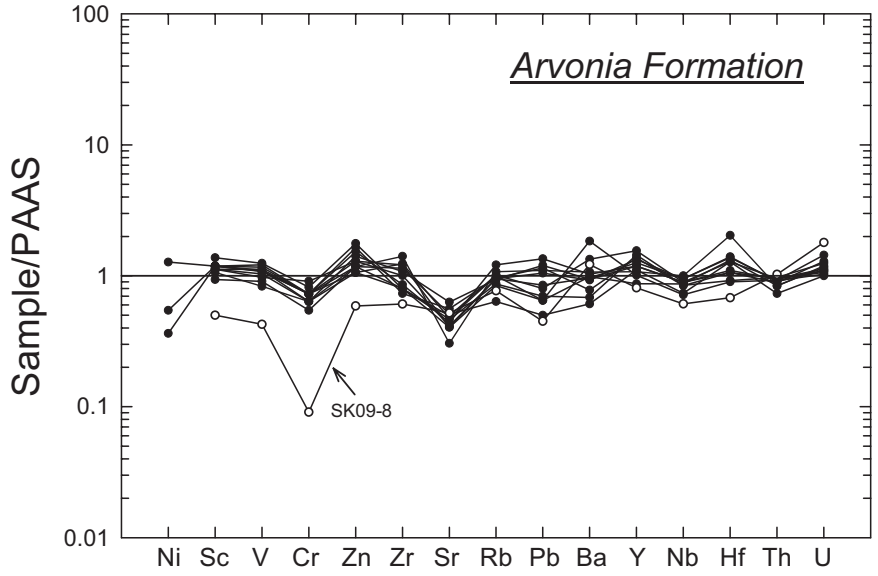

Fig. 6. Trace element compositions of Arvonia samples normalized to PAAS. Normalizing values from Taylor and McLennan (1985). For Ni, only those samples for which a value could be determined are plotted.

Nesbitt and Young (1982) is a commonly-used method for quantifying the degree of source area weathering. CIA values are calculated using the equation (in molecular proportions):

$$\mathrm{CIA} = [\mathrm{Al_2O_3}/(\mathrm{Al_2O_3} + \mathrm{CaO^*} + \mathrm{Na_2O} + \mathrm{K_2O})] \times 100$$

where CaO* represents the Ca in the silicate fraction only. For the Arvonia samples, we applied a correction for apatite to obtain CaO*, and for all samples the level of CaO is sufficiently low that no other correction (that is, for carbonate) is necessary. Fresh rocks typically have CIA values of about 50, whereas intensely weathered rocks yield values approaching 100 (reflecting complete conversion to kaolinite or gibbsite).

CIA values for Arvonia samples range from 67 to 78, reflecting an intermediate degree of weathering of the source area (Fedo and others, 1995). Although similar to the value for PAAS (70), ten of the twelve Arvonia samples have higher values, suggesting somewhat more intense weathering of the Arvonia source area.

The ternary $\mathrm{Al_2O_3} - (\mathrm{CaO^*} + \mathrm{Na_2O}) - \mathrm{K_2O}$ (A-CN-K) diagram of Nesbitt and Young (1984) is also useful for evaluating weathering trends as well as the effects of metasomatism accompanying diagenesis and weathering, particularly addition of K. Chemical weathering trends on this diagram typically parallel the A-CN sideline (reflecting plagioclase breakdown), and the point of intersection of the weathering trend line with the plagioclase—K-feldspar join provides some insights into the average source rock type (Fedo and others, 1995).

When plotted on this ternary, Arvonia compositions yield a linear array, albeit with some scatter (fig. 9A). Most samples plot closer to the A-K sideline than PAAS, again consistent with a greater degree of weathering of the Arvonia source area. An arrow (fitted by eye) through the data projects approximately to the composition of granodiorite or average upper continental crust (UCC). However, the weathering trend line in this case has a shallower slope than the predicted weathering trend for this composition, as shown on figure 9B. Fedo and others (1995) showed that such trends are

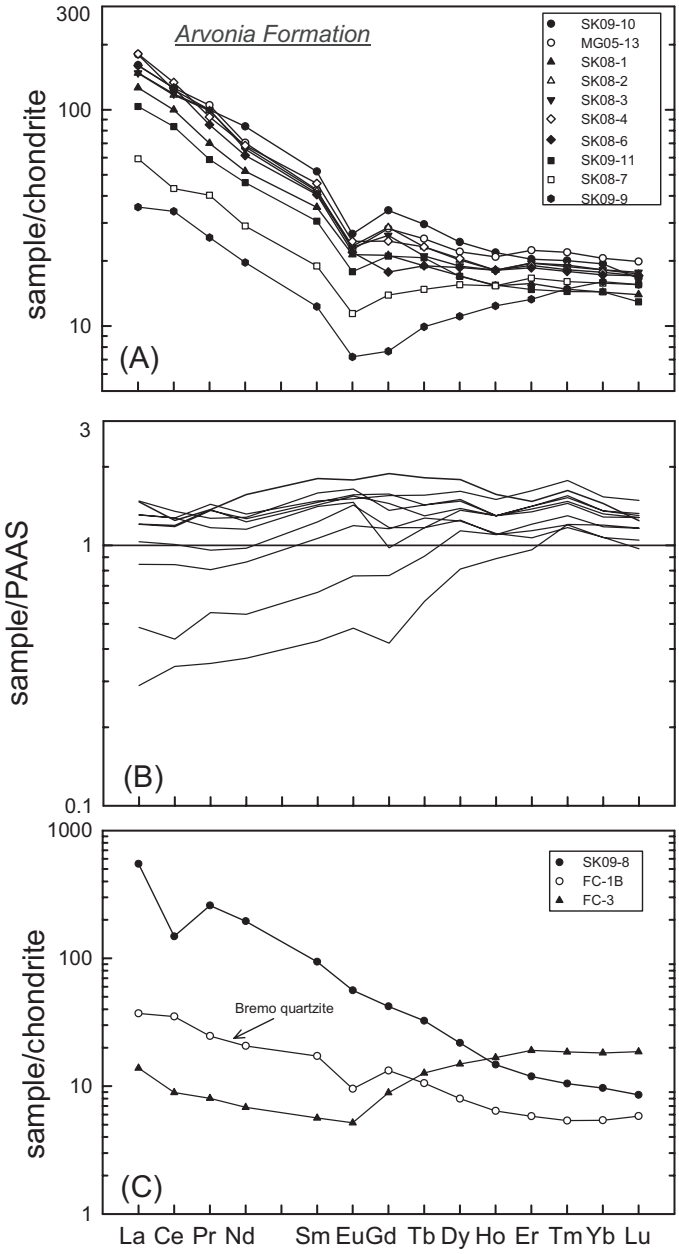

Fig. 7. Plots of chondrite- and PAAS-normalized concentrations of rare-earth elements (REE) in Arvonia Formation samples. (A) Plot of eight samples with similar patterns, and two (SK08-7, SK09-9) that show some depletion in the light and middle REE; (B) PAAS-normalized concentrations of the same samples in (A); (C) Chondrite-normalized plot of two samples with anomalous patterns (SK09-8, FC-3) and a single sample of Bremo quartzite (FC-1B). Chondrite normalizing values from Boynton (1984).

consistent with K-metasomatism during weathering, primarily reflecting illitization of kaolinite. Fedo and others (1995) illustrated a graphical method of correcting for this K-metasomatism, by projecting a line from the K-apex through the sample data point

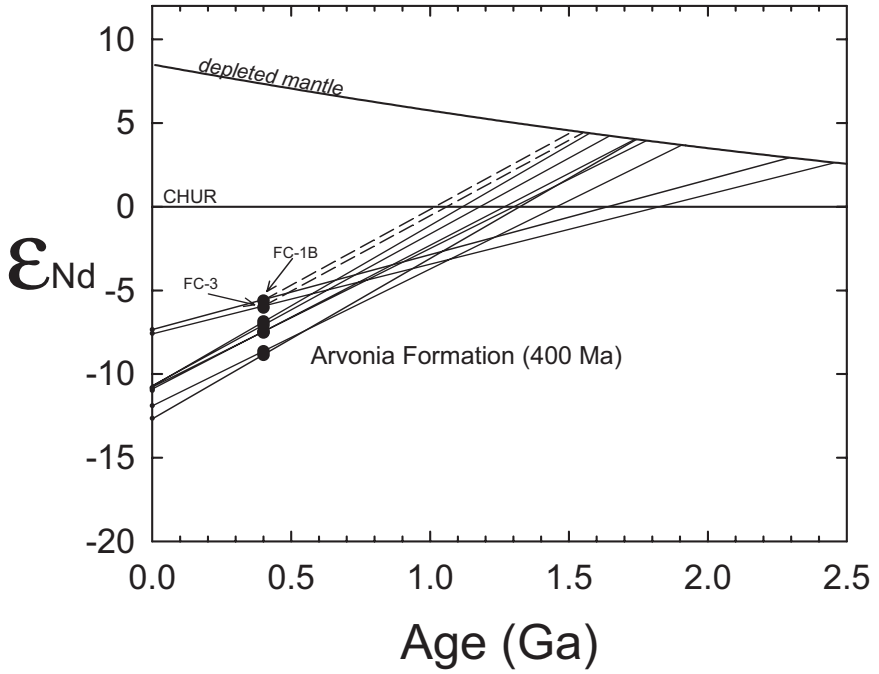

Fig. 8. A plot of initial ε_{Nd} vs. age for samples from the Arvonia Formation. Lines illustrate the change in ε_{Nd} with time. Dashed lines from FC-1B and FC-3 illustrate two-stage model ages (T_{DM2}) for these samples (see text for discussion). Depleted mantle curve is from DePaolo (1981). CHUR = chondritic uniform reservoir.

onto a line representing the normally predicted weathering trend. The point of intersection can then be used to estimate a revised CIA value from the vertical CIA axis. This approach for the Arvonia compositions is illustrated on figure 9B, where example projection lines for three samples are shown. Using this approach, corrected CIA values range from 68 to 89 (table 1), with ten samples having values ≥78. Values above 80 are indicative of extreme weathering conditions (Fedo and others, 1995). Thus, these revised values clearly indicate a higher degree of weathering of the Arvonia source area compared to that of PAAS.

These results suggest that subtropical to tropical climate conditions prevailed during weathering of the Arvonia source area, and imply a location near the equator. This interpretation is consistent with paleogeographic reconstructions that show that most of Laurentia was within 30° of the equator from the Middle Ordovician through the Devonian (for example, Condie and Sloan, 1998; Blakey, 2007). Some tropical areas are characterized by steady-state weathering conditions (a balance between chemical weathering and erosion rates), which result in a tight grouping of compositions on the A-CN-K diagram (Nesbitt and others, 1997). In contrast, the Arvonia compositions form a somewhat scattered linear array on figure 9. Nesbitt and others (1997) showed that such arrays reflect non-steady-state weathering conditions, in which rates of weathering and erosion are more variable. Non-steady-state conditions are more typical of regions that are either tectonically active or which experience more variable climate. In such settings, a spectrum of weathered zones may be eroded at once via mass wasting, producing sediments of variable composition (for example, Fedo and others, 1997).

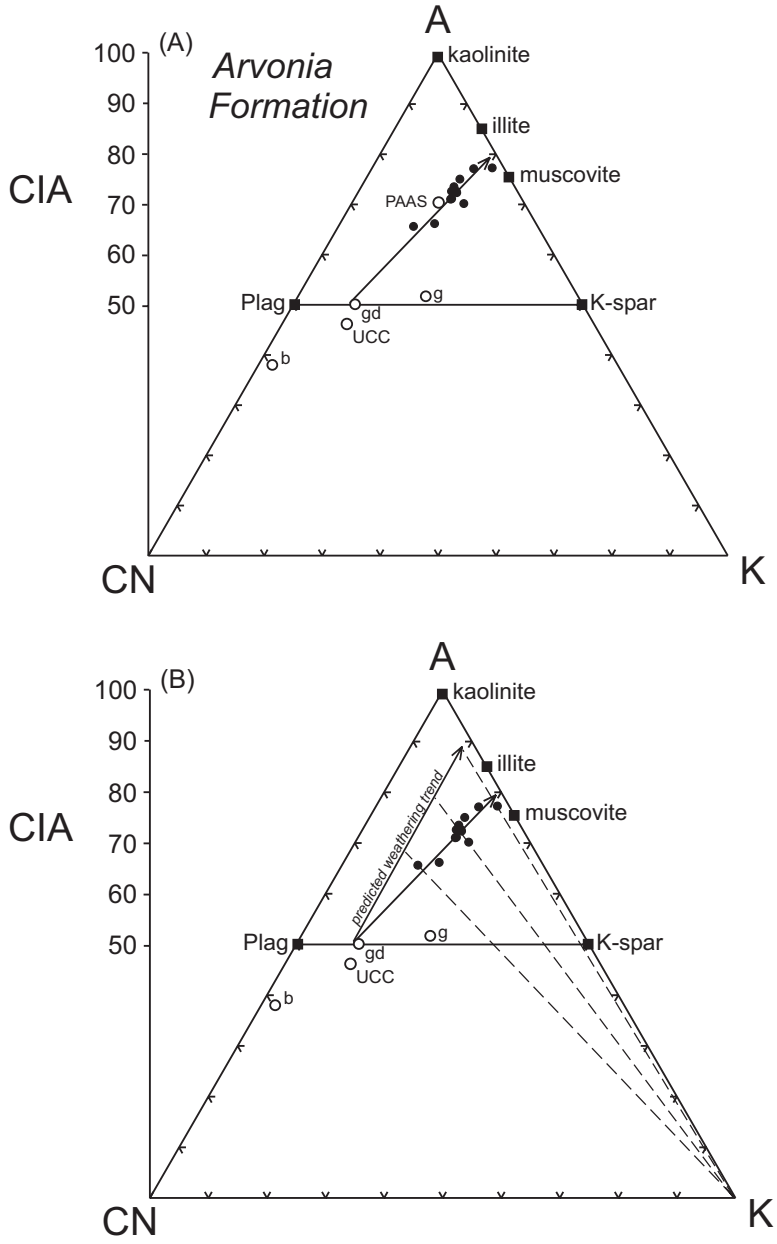

Fig. 9. (A) A-CN-K (Al_2O_3-CaO+Na_2O-K_2O) ternary diagram (Nesbitt and Young, 1984) showing Arvonia Formation samples. Shown for reference are positions for PAAS and Upper Continental Crust (UCC) (both from Taylor and McLennan, 1985), positions for average basalt (b), granodiorite (gd) and granite (g) (all from Nockolds, 1954), and various minerals. Vertical scale on the left is for Chemical Index of Alteration (CIA) values. Arrow shows a weathering trend line defined by the samples, which intersects the feldspar join at approximately the composition of granodiorite; (B) Same plot as in (A), but with the addition of: 1) the predicted weathering trend for this composition, which parallels the A-CN sideline; and 2) example lines (dashed) lines illustrating the method of correction for K-metasomatism (see text for discussion).

Diagenetic Effects

Eight of the twelve slate and schist samples have relatively uniform chondrite-normalized REE patterns (fig. 7A), suggesting little disturbance of their REE concentrations. However, three samples (SK08-7, SK09-9, and FC-3) display varying degrees of LREE depletion, and one (SK09-8) is anomalously LREE-enriched. It is now reasonably well established that some disturbance of original REE concentrations in shales, particularly the LREE, can occur at a variety of scales during diagenesis (for example, Awwiller and Mack, 1991; Milodowski and Zalasiewicz, 1991; Ohr and others, 1991, 1994; Lev and others, 1999; Chakrabarti and others, 2007). Such changes are typically attributed to dissolution/reprecipitation of trace amounts of REE-rich phosphates such as monazite, apatite, or rhabdophane. Evaluation of these disturbances is particularly important for the proper interpretation of Nd-isotopic results because they can result in anomalously old depleted mantle model ages (for example, Bock and others, 1994).

Bock and others (1994) utilized a plot of $f_{Sm/Nd}$ vs. $\varepsilon_{Nd}(t)$ to illustrate combined Nd-isotopic and REE abundance information. Values of $f_{Sm/Nd}$ reflect the $^{147}Sm/^{144}Nd$ ratio, that is, they provide an indication of the slope of the REE pattern between Nd and Sm. Such a plot for the Arvonia samples is shown in figure 10, where the data form a vertical array, albeit with some scatter. Bock and others (1994) showed that such arrays are consistent with REE disturbance at approximately the time of deposition or early diagenesis. Specifically, the Nd-isotopic compositions of the samples were the same at the time of deposition (reflected in their similar ε_{Nd} values), but the spread in $f_{Sm/Nd}$ values indicates some redistribution of the LREE. An interesting observation from figure 10 is that although samples SK08-7 and SK09-9 appear to have lost LREE relative to the majority of the samples, this loss did not result in any appreciable change in the Sm/Nd ratio. As shown, their $f_{Sm/Nd}$ values lie between the values for the rest of the samples.

Results of a modeling exercise designed to evaluate the loss of LREE in samples SK08-7, SK09-9, and FC-3 are shown on figure 11. We used the approach of McLennan and others (1995; see also Lev and others, 1999), which is essentially a mass balance calculation involving removal of a certain percentage of a LREE-enriched phase from the presumably unaltered composition to yield the altered composition. The abundances of the REE in the removed phase are determined by the mass of the removed material (McLennan and others, 1995). For samples SK08-7 and SK09-9, we used the Arvonia average (of the eight similar patterns) for the unaffected composition. Results of some example calculations are shown in the upper portion of figure 11, which show the REE patterns of a hypothetical LREE-enriched phase, assuming removal of the percentages shown. Loss of only 0.1 percent and 0.13 percent of such a phase can account for the change from the Arvonia average to the compositions of SK08-7 and SK09-9, respectively. For sample FC-3, it is inappropriate to use the Arvonia average because this sample has HREE concentrations that are higher than the average. In this case, we used the most enriched Arvonia composition (Arvonia high) as a starting point, and the result for removal of 0.19 percent of the LREE-enriched phase is shown. The REE concentrations and patterns for the hypothetical removed phase are obviously like those of monazite. Thus, a plausible interpretation for the rotated patterns of these three samples, particularly FC-3, is that they reflect diagenetic loss of a small amount of monazite.

Sample SK09-8 presents the opposite situation in that it is LREE-enriched relative to the unaltered samples. A simple explanation for this enrichment could be addition of a small amount of monazite. For example, addition of ~0.3 to 0.4 percent of one of the LREE-enriched phases in the models above to the average composition is sufficient to reproduce the concentrations and patterns of the LREE in SK09-8. However, this

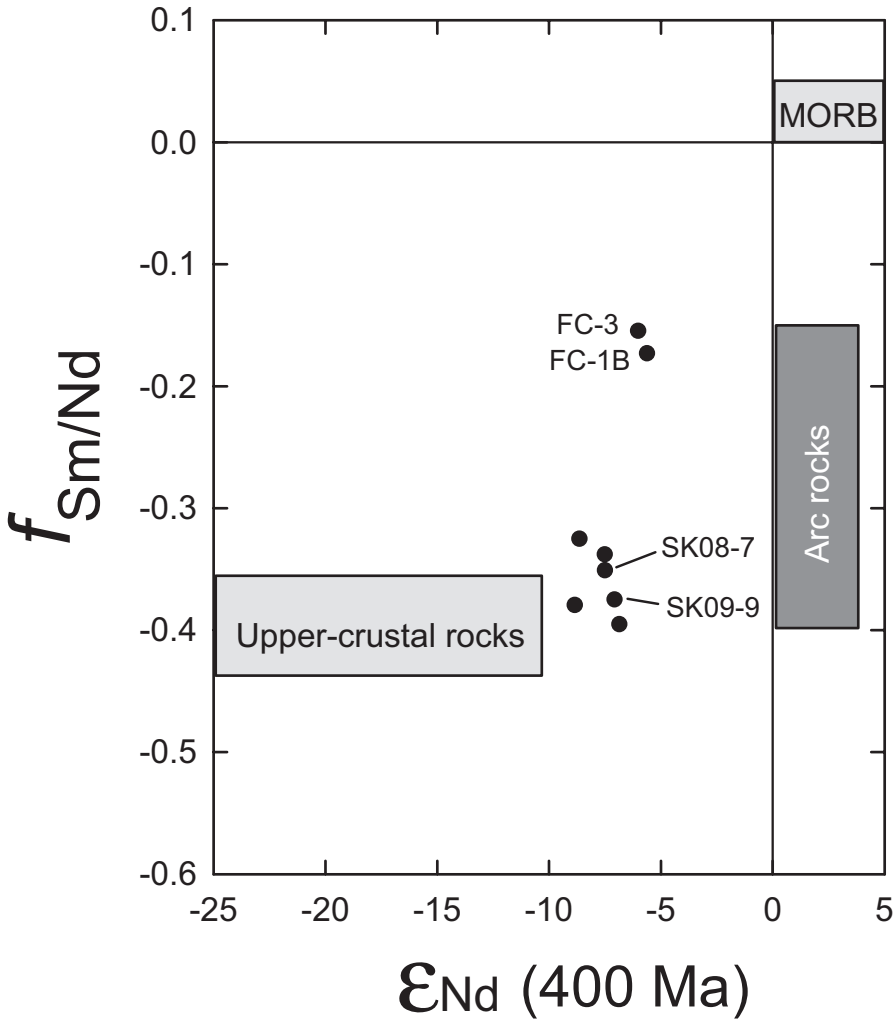

Fig. 10. A plot of ε_{Nd} vs. $f_{Sm/Nd}$ for Arvonia Formation samples. Fields for upper-crustal rocks, arc rocks, and mid-ocean ridge basalt (MORB) are from Bock and others (1994).

addition results in HREE concentrations that are too high, because this sample is HREE-depleted relative to the rest. This depletion could reflect some sedimentary sorting of zircon, and this sample does have the lowest Zr content. Coupled with the pronounced negative Ce-anomaly, these observations suggest a complicated history of REE redistribution in this sample that cannot be uniquely modeled.

Additional support for the timing of LREE redistribution in these rocks comes from the good correlation (r^2=0.98) between $^{147}Sm/^{144}Nd$ and T_{DM} values, as shown on figure 12. Lev and others (1999; see also Bock and others, 2004) noted that such positive correlations are consistent with LREE disturbance at approximately the time of deposition. An additional and important implication of the distribution of data points on figure 12 is that most samples have undergone some degree of LREE disturbance, such that their model ages are also anomalously old. Indeed, the

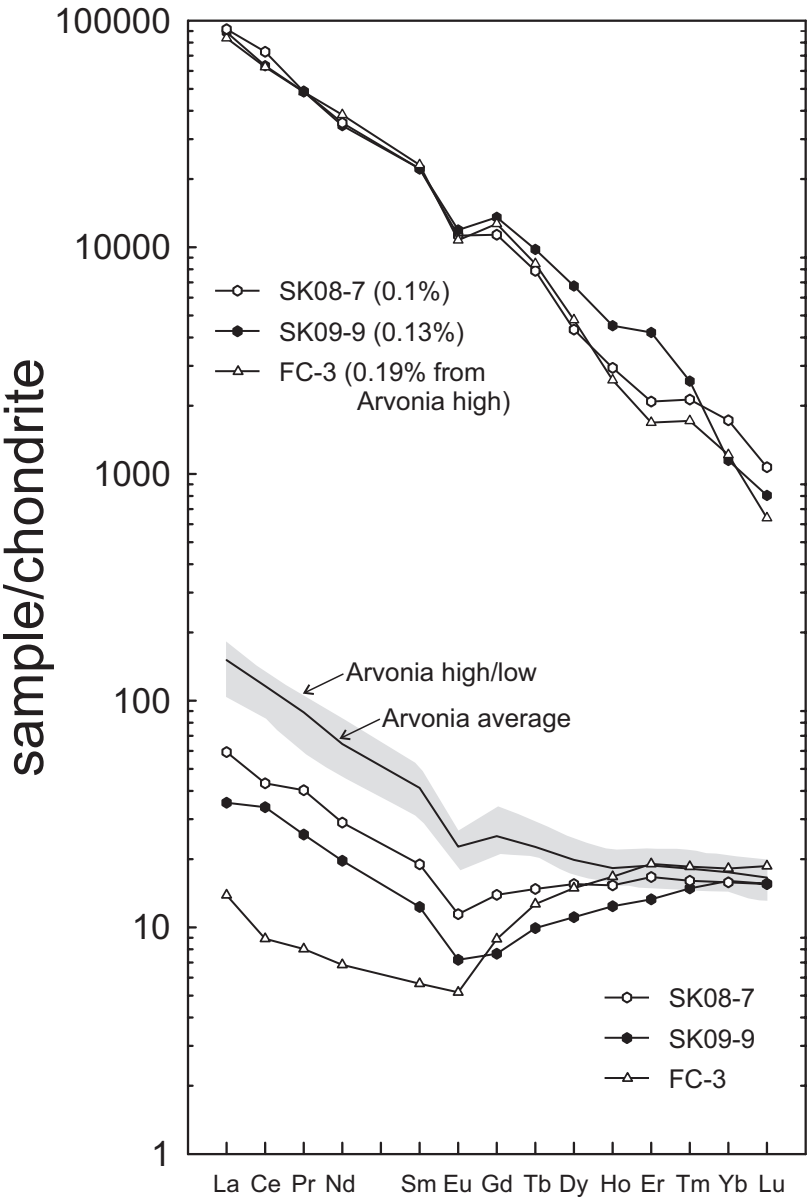

Fig. 11. Chondrite-normalized REE diagram comparing three of the LREE-depleted samples with the average and range of the other Arvonia samples (sample SK09-8 is not included in this group). REE concentrations in samples SK08-7 and SK09-9 can be explained by removal of LREE from the Arvonia average; sample FC-3 can be similarly explained by loss of LREE from the Arvonia high composition. Also shown in the upper part of the diagram are REE patterns for the removed material for each sample, calculated using the percentages shown. See text for additional discussion.

$^{147}Sm/^{144}Nd$ values of most samples are higher than is typical for unaltered shales [0.10-0.12; Taylor and McLennan (1985)]. This result highlights the potential problems in using model ages to infer provenance information.

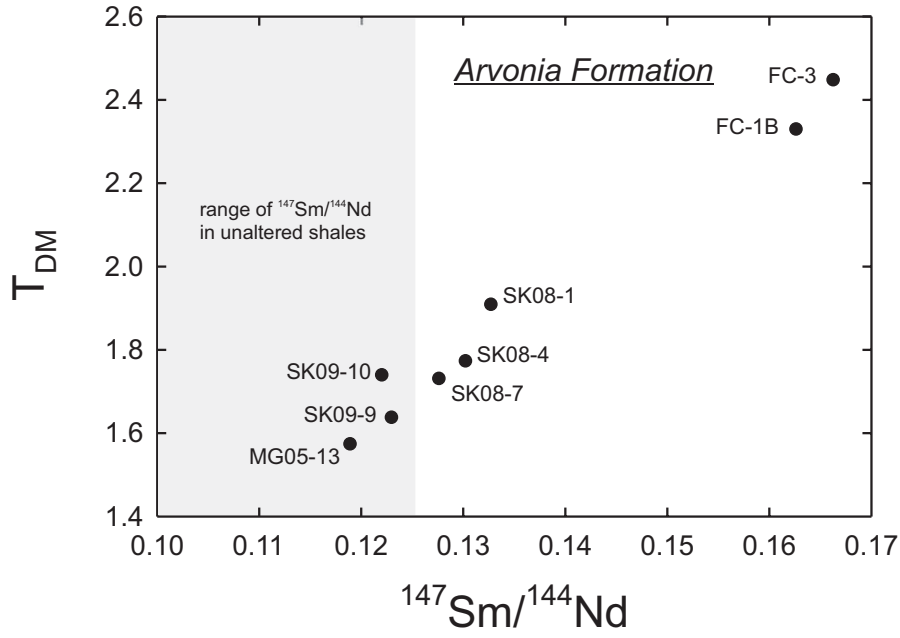

Fig. 12. A plot of $^{147}Sm/^{144}Nd$ vs. depleted mantle model ages (T_{DM}) for Arvonia Formation samples. The clear positive correlation indicates some disturbance of the LREE for most samples at approximately the time of deposition, such that the model ages for most are anomalously old. Shaded field shows the range in $^{147}Sm/^{144}Nd$ values in typical unaltered shales (Taylor and McLennan, 1985).

Provenance Type

McLennan and others (1993, 1995) used whole-rock chemical and Nd-isotopic compositions to define five distinct provenance components or terrane types, including Old Upper Continental Crust, Recycled Sedimentary Rocks, Young Undifferentiated Arc, Young Differentiated Arc, and Exotic Components (for example, ophiolites). Of these five, Arvonia compositions are most similar to the Old Upper Continental Crust provenance type. This type is characterized by: 1) generally negative $\varepsilon_{Nd}(t)$ values; 2) Eu/Eu* $\sim$ 0.6-0.7; 3) Th/Sc $\sim$ 1.0; 4) Th/U $>$ 3.8; and Rb/Sr $>$ 0.5. The Arvonia compositions match these characteristics reasonably well, although there are some contrasts.

Figure 13 illustrates some key immobile trace element ratios (Zr/Sc, Th/Sc, Th/U) in the Arvonia samples, and how they compare with various reference compositions. These ratios and plots are useful for assessing provenance bulk composition as well as the roles of weathering and sedimentary recycling in controlling the composition of the original sediments (McLennan and others, 1993). As described by McLennan and others (1993), the Th/Sc ratio is a sensitive monitor of provenance bulk composition (mafic vs. felsic), whereas Zr/Sc ratios tend to increase with increasing degrees of sediment recycling. The Arvonia compositions form a narrow cluster on figure 13A, with similar Th/Sc values for all samples [average = 0.71 $\pm$ 0.08 (2SD)] (sample SK09-8 is an obvious exception, with a higher value that stems from what seems to be an anomalously low Sc concentration). Values for Zr/Sc vary only by about a factor of 2, from 7.6 to 17.4. The minimal variation in Th/Sc values indicates that the Arvonia sediments were derived from a well-mixed source, or a single homogeneous source. The fact that the values are somewhat less than those for upper continental

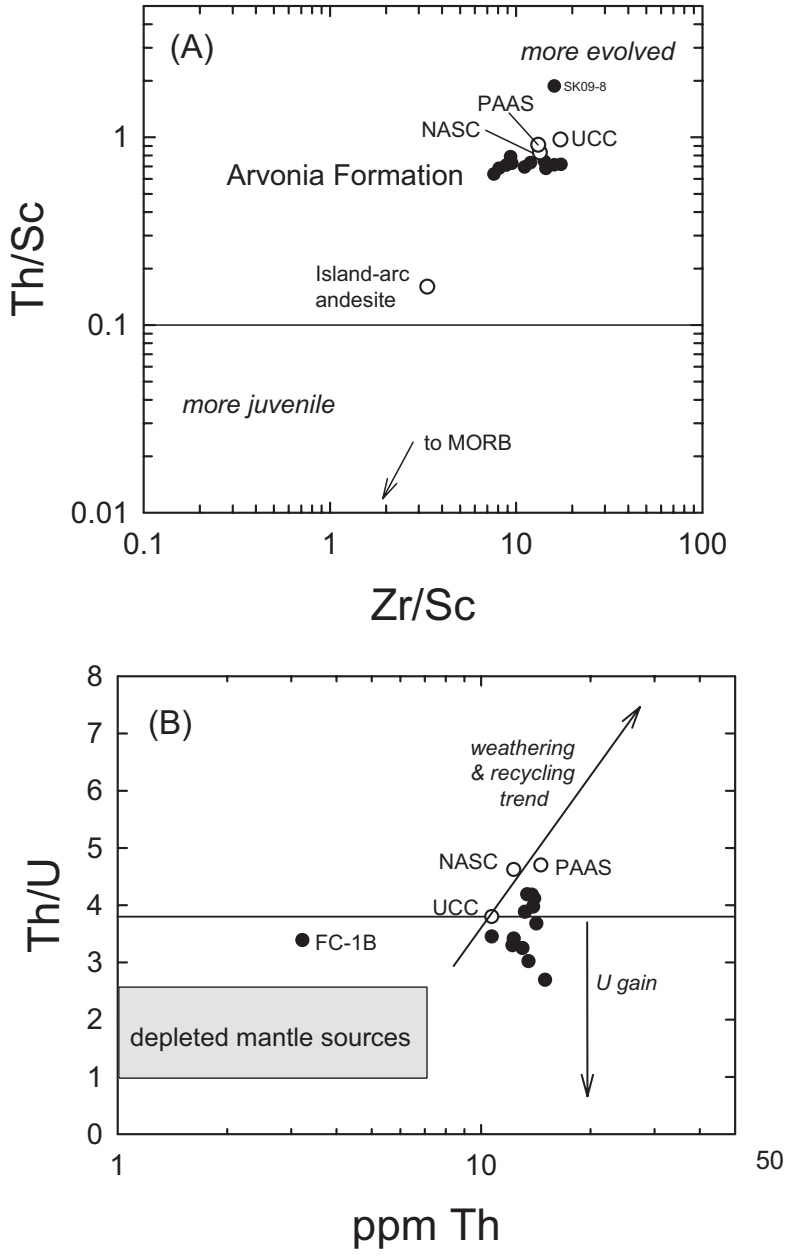

Fig. 13. (A) A plot of Zr/Sc vs. Th/Sc for Arvonia Formation samples (modified after McLennan and others, 1993). Also shown for reference are positions for UCC, PAAS, the North American Shale Composite (NASC; Gromet and others, 1984), and island-arc andesite (Taylor and McLennan, 1985); (B) Plot of ppm Th vs. Th/U for Arvonia samples (also after McLennan and others, 1993).

crust (UCC), the North American Shale Composite (NASC), and PAAS may reflect a contribution from a somewhat more mafic source or sources. Concentrations of Sc are in fact slightly higher in most Arvonia samples compared to the reference compositions, but Th values are similar. The relatively small variation in Zr/Sc values, along

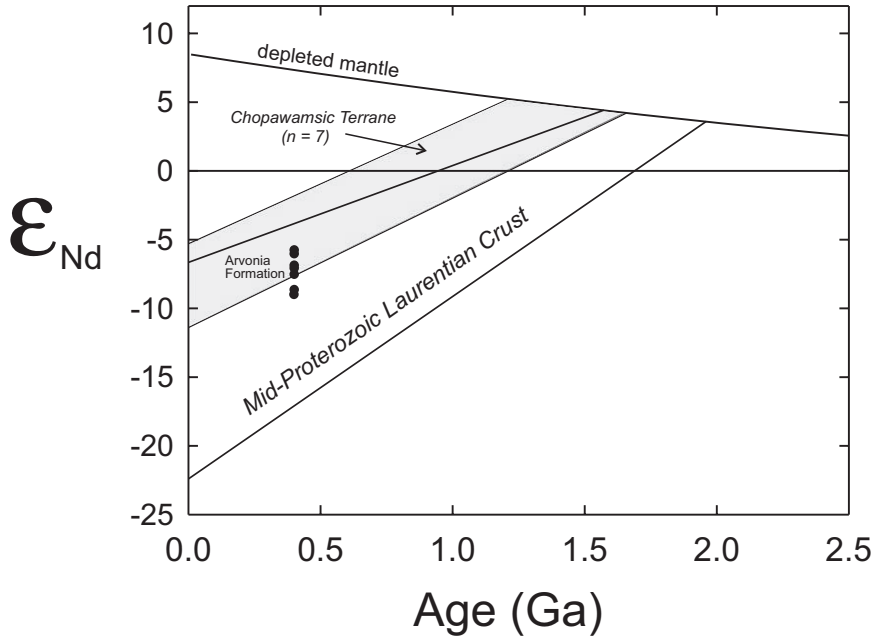

Fig. 14. A plot of initial ε_{Nd} vs. age for samples from the Arvonia Formation, along with fields for Mid-Proterozoic Laurentian crust and the Chopawamsic terrane (shaded). Laurentian crust field is generalized based on data in Pettingill and others (1984), Patchett and Ruiz (1989), Daly and McLelland (1991), McLelland and others (1993), Fullagar and others (1997), Smith and others (1997), Carrigan and others (2003), Ownby and others (2003), and Owens and Samson (2004). Field for the Chopawamsic terrane is based on data in Coler and others (2000).

with Th/Sc values <1, indicates a minimal role for sedimentary recycling in the origin of the Arvonia sediments.

This interpretation regarding the effects of sedimentary recycling is also supported by Th/U values, as illustrated on figure 13B. Prolonged weathering and recycling tend to result in increasing Th/U values as U^{4+} is oxidized to the more mobile U^{6+} (McLennan and others, 1993), as shown by the arrow on figure 13B. Values of Th/U for the Arvonia samples cluster near or are less than the value for UCC (3.8), and are less than those for both NASC and PAAS. Such values are consistent with a limited role for sedimentary recycling, although weathering under more reducing conditions compared to NASC or PAAS could also result in less loss of U.

Constraints From Nd-Isotopic Compositions

The Nd-isotopic compositions of Arvonia rocks reinforce the interpretation of sediment sources dominated by an old, upper crustal provenance type. Specifically, the negative $\varepsilon_{Nd}(t)$ values for all samples require a source characterized by long-term LREE enrichment. The most obvious candidate source material of this type is Laurentian crust to the west. Figure 14 is an ε_{Nd} versus age plot of Arvonia compositions that includes a field for Mid-Proterozoic Laurentian crust. The Arvonia compositions lie well within this field, consistent with derivation from Laurentia.

Of perhaps greater significance is the fact that the $\varepsilon_{Nd}(t)$ values for the Arvonia samples (-5.6 to -8.9) are essentially the same as those of post-450 Ma sedimentary rocks throughout North America. As documented by Patchett and others (1999; compare Gleason and others, 1994, 1995), sedimentary rocks across North America

show a pronounced shift in Nd-isotopic composition at ~450 Ma, from more negative $\varepsilon_{Nd}(t)$ values (−12 to −26) to less negative values (−5 to −13). Patchett and others (1999) interpreted this shift to reflect the overwhelming influence of sediments derived from the Caledonian-Appalachian mountains throughout the Paleozoic following the Taconic Orogeny. The isotopic signature of those sediments [$\varepsilon_{Nd}(t)$ values from −5 to −13; T_{DM} values from 1.0-1.6 Ga] reflects derivation from the Grenville Orogenic belt, that is, Mid-Proterozoic Laurentia. In addition, Gleason and others (1994, 1995, 2002) defined an "Appalachian type" signature for post-Middle Ordovician sedimentary rocks that is characterized by $\varepsilon_{Nd}(t)$ values between −7 and −9 (averaging −8), and with T_{DM} = 1.4–1.7 Ga. Despite the complications described above regarding model ages for the Arvonia rocks, their Nd-isotopic compositions are clearly consistent with derivation from such an Appalachian source.

Given their unconformable position above older rocks of the Chopawamsic terrane, it is plausible that these rocks also contributed to the Arvonia sediments. Also shown on figure 14 is a shaded field for Chopawamsic rocks, based on a limited data set (Coler and others, 2000). All but two of the Arvonia samples fall within this field, so derivation of Arvonia sediments either wholly or in part from older Chopawamsic rocks is at least permissible. This interpretation implies that the Chopawamsic terrane has both chemical and isotopic characteristics similar to old cratonal sources. This view may be valid as the Chopawamsic arc terrane is known to be quite evolved, not just because of its evolved Nd isotopic composition but also because of the presence of Proterozoic zircon xenocrysts in many volcanic rocks (Coler and others, 2000). A further connection between the Arvonia Formation and the Chopawamsic terrane is the abundance of 470 to 400 Ma detrital zircon in basal quartzites of the Arvonia Formation (Bailey and others, 2008). That age range encompasses the crystallization ages of both volcanic and plutonic units of the Chopawamsic terrane (Coler and others, 2000; Aleinikoff and others, 2002; Horton and others, 2010). Another possibility is that the Arvonia Formation is indeed a successor basin that formed following accretion of the Chopawamsic arc, but that any juvenile material in the arc contributed little to the sedimentary basin.

The ultimate origin of the Chopawamsic terrane, either as a peri-Laurentian or peri-Gondwanan arc, is still debated. Based on the presence of Mesoproterozoic (1.3-1.0 Ga) zircon xenocrysts in an Ordovician rhyolite from the terrane (Coler and others, 2000), one might favor the interpretation of a Laurentian origin as rocks of this age are so abundant in eastern Laurentia. If that view is correct, and if the Chopawamsic terrane was a major sedimentary source of Arvonia Formation sediments as we suggest in this study, then Arvonia rocks are also not exotic. However, it is clear that further chronological and isotopic characterization of Chopawamsic and overlying rocks is warranted before any more definitive answers can be offered concerning ultimate paleogeographic origins.

ACKNOWLEDGMENTS

A portion of this work was completed by Sarah King for her undergraduate thesis at the College of William and Mary, and we acknowledge some financial support from the College. We also thank various land and quarry owners for access to their properties. Scott McLennan provided some helpful insights during the early stages of this project. Finally, we thank Chris Fedo and Steven Lev for highly constructive journal reviews.

References

Aleinikoff, J. N., Horton, J. W., Jr., Drake, A. A., Jr., and Fanning, C. M., 2002, SHRIMP and conventional U-Pb ages of Ordovician granites and tonalites in the central Appalachian Piedmont: Implications for

Paleozoic tectonic events: American Journal of Science, v. 302, n. 1, p. 50–75, http://dx.doi.org/10.2475/ajs.302.1.50
Awwiller, D. N., and Mack, L. E., 1991, Diagenetic modification of Sm-Nd model ages in Tertiary sandstones and shales, Texas Gulf Coast: Geology, v. 19, n. 4, p. 311–314, http://dx.doi.org/10.1130/0091-7613(1991)019⟨0311:DMOSNM⟩2.3.CO;2
Bailey, C. M., Eriksson, K., Allen, C., and Campbell, I., 2008, Detrital zircon geochronology of the Chopawamsic terrane, Virginia Piedmont: evidence for a non-Laurentian provenance: Geological Society of America Abstracts with Programs, v. 40, n. 6, p. 451.
Blakey, R. C., 2007, Carboniferous-Permian paleogeography of the assembly of Pangaea, *in* Wong, Th. E., editor, Proceedings of the XVth International Congress on Carboniferous and Permian stratigraphy: Utrecht, Royal Netherlands Academy of Arts and Sciences, p. 443–456.
Bock, B., McLennan, S. M., and Hanson, G. N., 1994, Rare earth element redistribution and its effects on the neodymium isotope system in the Austin Glen Member of the Normanskill Formation, New York, USA: Geochimica et Cosmochimica Acta, v. 58, n. 23, p. 5245–5253, http://dx.doi.org/10.1016/0016-7037(94)90308-5
Bock, B., Hurowitz, J. A., McLennan, S. M., and Hanson, G. N., 2004, Scale and timing of rare earth element redistribution in the Taconian foreland of New England: Sedimentology, v. 51, n. 4, p. 885–897, http://dx.doi.org/10.1111/j.1365-3091.2004.00656.x
Boynton, W. V., 1984, Geochemistry of the rare earth elements: meteorite studies, *in* Henderson, P., editor, Rare Earth Element Geochemistry: New York, Elsevier, p. 63–114.
Brown, W. R., 1969, Geology of the Dillwyn Quadrangle, Virginia: Virginia Division of Mineral Resources, Report of Investigations 10, 77 p.
——— 1986, Shores Complex and melange in the central Virginia Piedmont: Geological Society of America Centennial Field Guide—Southeastern Section, v. 6, p. 209–214.
Carrigan, C. W., Miller, C. F., Fullagar, P. D., Hatcher, R. D., Jr., Bream, B. R., and Coath, C. D., 2003, Ion microprobe age and geochemistry of southern Appalachian basement, with implications for Proterozoic and Paleozoic reconstructions: Precambrian Research, v. 120, n. 1–3, p. 1–36, http://dx.doi.org/10.1016/S0301-9268(02)00113-4
Chakrabarti, R., Abanda, P. A., Hannigan, R. E., and Basu, A. R., 2007, Effects of diagenesis on the Nd-isotopic composition of black shales from the 420 Ma Utica shale magnafacies: Chemical Geology, v. 244, n. 1–2, p. 221–231, http://dx.doi.org/10.1016/j.chemgeo.2007.06.017
Coler, D. G., Wortman, G. L., Samson, S. D., Hibbard, J. P., and Stern, R., 2000, U-Pb geochronologic, Nd isotopic, and geochemical evidence for the correlation of the Chopawamsic and Milton Terranes, Piedmont Zone, Southern Appalachian orogen: Journal of Geology, v. 108, n. 4, p. 363–380, http://dx.doi.org/10.1086/314411
Condie, K. C., and Sloan, R. E., 1998, Origin and Evolution of Earth: Principles of Historical Geology: Upper Saddle River, New Jersey, Prentice Hall, 498 p.
Conley, J. F., and Marr, J. M., Jr., 1980, Evidence for the correlation of the kyanite quartzites of Willis and Woods mountains with the Arvonia Formation, *in* Contributions to Virginia Geology—IV: Virginia Division of Mineral Resources Publication 27, p. 1–11.
Couture, R. A., and Dymek, R. F., 1996, A reexamination of absorption and enhancement effects in X-ray fluorescence trace element analysis: American Mineralogist, v. 81, n. 5–6, p. 639–650.
Couture, R. A., Smith, M. S, and Dymek, R. F., 1993, X-ray fluorescence analysis of silicate rocks using fused glass discs and a side window Rh tube: accuracy, precision and reproducibility: Chemical Geology, v. 110, n. 4, p. 315–328, http://dx.doi.org/10.1016/0009-2541(93)90326-E
Daly, J. S., and McLelland, J. M., 1991, Juvenile Middle Proterozoic crust in the Adirondack Highlands, Grenville province, northeastern North America: Geology, v. 19, n. 2, p. 119–122, http://dx.doi.org/10.1130/0091-7613(1991)019⟨0119:JMPCIT⟩2.3.CO;2
Darton, N. H., 1892, Fossils in the "Archean" rocks of central Piedmont, Virginia: American Journal of Science, v. 44, p. 50–52.
DePaolo, D. J., 1981, Neodymium isotopes in the Colorado Front Range and crust-mantle evolution in the Proterozoic: Nature, v. 291, p. 193–196, http://dx.doi.org/10.1038/291193a0
Diecchio, R., and Gottfried, R., 2004, Regional tectonic history of northern Virginia, *in* Southworth, S., and Burton, W., editors, Geology of the National Capital Region—Field Trip Guidebook: United States Geological Survey Circular 1264, p. 1–14.
Dorsch, J., 1992, Extensional basin formation during collapse of the Taconic orogen: a hypothesis for the Arvonia and Quantico successor basins of the central Appalachian Piedmont: Geological Society of America Abstracts with Programs, v. 24, n. 3, p. 17.
Dymek, R. F., and Owens, B. E., 2001, Chemical assembly of Archaean anorthosites from amphibolite- and granulite-facies terranes, SW Greenland: Contributions to Mineralogy and Petrology, v. 141, n. 5, p. 513–528, http://dx.doi.org/10.1007/s004100100264
Evans, N. H., ms, 1984, Latest Precambrian to Ordovician metamorphism and orogenesis in the Blue Ridge and western Piedmont, Virginia Appalachians: Blacksburg, Virginia, Virginia Tech, Ph.D. thesis, 322 p.
Evans, N. H., and Marr, J. D., Jr., 1988, Geology and the slate industry in the Arvonia District, Buckingham County, Virginia: Virginia Minerals, v. 34, p. 37–44.
Fedo, C. M., Nesbitt, H. W., and Young, G. M., 1995, Unraveling the effects of potassium metasomatism in sedimentary rocks and paleosols, with implications for paleoweathering conditions and provenance: Geology, v. 23, n. 10, p. 921–924, http://dx.doi.org/10.1130/0091-7613(1995)023⟨0921:UTEOPM⟩2.3.CO;2
Fedo, C. M., Young, G. M., and Nesbitt, H. W., 1997, Paleoclimatic control on the composition of the Paleoproterozoic Serpent Formation, Huronian Supergroup, Canada: a greenhouse to icehouse

transition: Precambrian Research, v. 86, n. 3–4, p. 201–223, http://dx.doi.org/10.1016/S0301-9268(97)00049-1

Fullagar, P. D., Goldberg, S. A., and Butler, J. R., 1997, Nd and Sr isotopic characterization of crystalline rocks from the southern Appalachian Piedmont and Blue Ridge, North and South Carolina, *in* Sinha, A. K., Whalen, J. B., and Hogan, J. P., editors, The Nature of Magmatism in the Appalachian Orogen: Geological Society of America Memoir 191, p. 165–179, http://dx.doi.org/10.1130/0-8137-1191-6.165

Garver, J. I., and Scott, T. J., 1995, Trace elements in shale as indicators of crustal provenance and terrane accretion in the southern Canadian Cordillera: Geological Society of America Bulletin, v. 107, p. 440–453, http://dx.doi.org/10.1130/0016-7606(1995)107⟨0440:TEISAI⟩2.3.CO;2

Gleason, J. D., Patchett, P. J., Dickinson, W. R., and Ruiz, J., 1994, Nd isotopes link Ouachita turbidites to Appalachian sources: Geology, v. 22, n. 4, p. 347–350, http://dx.doi.org/10.1130/0091-7613(1994)022⟨0347:NILOTT⟩2.3.CO;2

——— 1995, Nd isotopic constraints on sediment sources of the Ouachita-Marathon fold belt: Geological Society of America Bulletin, v. 107, n. 10, p. 1192–1210, http://dx.doi.org/10.1130/0016-7606(1995)107⟨1192:NICOSS⟩2.3.CO;2

Gleason, J. D., Finney, S. C., and Gehrels, G. E., 2002, Paleotectonic implications of a Mid- to Late-Ordovician provenance shift, as recorded in sedimentary strata of the Ouachita and southern Appalachian mountains: Journal of Geology, v. 110, n. 3, p. 291–304, http://dx.doi.org/10.1086/339533

Glover, L., III, Evans, N. H., Patterson, J. G., and Brown, W. R., 1989, Tectonics of the Virginia Blue Ridge and Piedmont, Culpeper to Richmond, Virginia, *in* Metamorphism and Tectonics of eastern and central North America: American Geophysical Union, 28th International Geological Congress, v. 3, Field Trip Guidebook T363, 59 p.

Gromet, L. P., Dymek, R. F., Haskin, L. A., and Korotev, R. L., 1984, The "North American shale composite": its compilation, major and trace element characteristics: Geochimica et Cosmochimica Acta, v. 48, n. 12, p. 2469–2482, http://dx.doi.org/10.1016/0016-7037(84)90298-9

Herron, M. M., 1988, Geochemical classification of terrigenous sands and shales from core or log data: Journal of Sedimentary Petrology, v. 58, n. 5, p. 820–829, http://dx.doi.org/10.1306/212F8E77-2B24-11D7-8648000102C1865D

Hibbard, J. P., van Staal, C. R., and Rankin, D. W., 2007, A comparative analysis of pre-Silurian crustal building blocks of the northern and the southern Appalachian orogen: American Journal of Science, v. 307, n. 1, p. 23–45, http://dx.doi.org/10.2475/01.2007.02

Horton, J. W., Jr., Aleinikoff, J. N., Drake, A. A., Jr., and Fanning, C. M., 2010, Ordovician volcanic arc-terrane in the Central Appalachian Piedmont of Maryland and Virginia: SHRIMP U-Pb geochronology, field relations, and tectonic significance, *in* Tollo, R. P., Bartholomew, M. J., Hibbard, J. P., and Karabinos, P. M., editors, From Rodinia to Pangea: the Lithotectonic Record of the Appalachian Region: Geological Society of America Memoir 206, p. 621–660, http://dx.doi.org/10.1130/2010.1206(25)

Kolata, D. R., and Pavlides, L., 1986, Echinoderms from the Arvonia Slate, central Virginia Piedmont: Geologica Et Palaeontologica, v. 20, p. 1–9.

Lev, S. M., McLennan, S. M., and Hanson, G. N., 1999, Mineralogic controls on REE mobility during black shale diagenesis: Journal of Sedimentary Research, v. 69, n. 5, p. 1071–1082, http://dx.doi.org/10.2110/jsr.69.1071

McLelland, J. M., Daly, J. S., and Chiarenzelli, J., 1993, Sm-Nd and U-Pb isotopic evidence of juvenile crust in the Adirondack Lowlands and implications for the evolution of the Adirondack Mts.: Journal of Geology, v. 101, n. 1, p. 97–105, http://dx.doi.org/10.1086/648198

McLennan, S. M., Hemming, S., McDaniel, D. K., and Hanson, G. N., 1993, Geochemical approaches to sedimentation, provenance, and tectonics, *in* Johnson, M. J., and Basu, A., editors, Processes controlling the composition of clastic sediments: Geological Society of America Special Paper 284, p. 21–40.

McLennan, S. M., Hemming, S. R., Taylor, S. R., and Eriksson, K. A., 1995, Early Proterozoic crustal evolution: geochemical and Nd-Pb isotopic evidence from metasedimentary rocks, southwestern North America: Geochimica et Cosmochimica Acta, v. 59, n. 6, p. 1153–1177, http://dx.doi.org/10.1016/0016-7037(95)00032-U

McLennan, S. M., Bock, B., Hemming, S. R., Hurowitz, J. A., Lev, S. M., and McDaniel, D. K., 2003, The roles of provenance and sedimentary processes in the geochemistry of sedimentary rocks, *in* Lentz, D. R., editor, Geochemistry of Sediments and Sedimentary Rocks: Evolutionary Considerations to Mineral Deposit-Forming Environments: Geological Association of Canada, GeoText 4, p. 7–38.

Milodowski, A. E., and Zalasiewicz, J. A., 1991, Redistribution of rare earth elements during diagenesis of turbidite/hemipelagite mudrock sequences of Llandovery age from central Wales, *in* Morton, A. C., Todd, S. P., and Haughton, P. D. W., editors, Developments in Sedimentary Provenance Studies: Geological Society Special Publication 57, p. 101–124.

Nesbitt, H. W., and Young, G. M., 1982, Early Proterozoic climates and plate motions inferred from major element chemistry of lutites: Nature, v. 299, p. 715–717, http://dx.doi.org/10.1038/299715a0

——— 1984, Prediction of some weathering trends of plutonic and volcanic rocks based on thermodynamic and kinetic considerations: Geochimica et Cosmochimica Acta, v. 48, n. 7, p. 1523–1534, http://dx.doi.org/10.1016/0016-7037(84)90408-3

Nesbitt, H. W., Fedo, C. M., and Young, G. M., 1997, Quartz and feldspar stability, steady and non-steady-state weathering and petrogenesis of siliciclastic sands and muds: Journal of Geology, v. 105, n. 2, p. 173–191, http://dx.doi.org/10.1086/515908

Nockolds, S. R., 1954, Average chemical compositions of some igneous rocks: Geological Society of America Bulletin, v. 65, n. 10, p. 1007–1032, http://dx.doi.org/10.1130/0016-7606(1954)65[1007:ACCOSI]2.0.CO;2

Ohr, M., Halliday, A. N., and Peacor, D. R., 1991, Sr and Nd isotopic evidence for punctuated clay diagenesis,

Texas Gulf Coast: Earth and Planetary Science Letters, v. 105, n. 1–3, p. 110–126, http://dx.doi.org/10.1016/0012-821X(91)90124-Z

——— 1994, Mobility and fractionation of rare earth elements in argillaceous sediments: Implications for dating diagenesis and low-grade metamorphism: Geochimica et Cosmochimica Acta, v. 58, n. 1, p. 289–312, http://dx.doi.org/10.1016/0016-7037(94)90465-0

Owens, B. E., and Pasek, M. A., 2007, Kyanite quartzites in the Piedmont Province of Virginia: evidence for a possible high-sulfidation system: Economic Geology, v. 102, n. 3, p. 495–509, http://dx.doi.org/10.2113/gsecongeo.102.3.495

Owens, B. E., and Samson, S. D., 2004, Nd-isotopic constraints on the magmatic history of the Goochland Terrane, easternmost Grenville crust in the southern Appalachians, *in* Tollo, R. P., Corriveau, L., McLelland, J. B., and Bartholomew, M. J., editors, Proterozoic Tectonic Evolution of the Grenville Orogen in North America: Geological Society of America Memoir 197, p. 601–608, http://dx.doi.org/10.1130/0-8137-1197-5.601

Owens, B. E., and Uschner, N. E., 2001, Mineralogy and geochemistry of metamorphosed ultramafic rocks in the central Piedmont Province of Virginia, *in* Raymond, L. A., and Warner, R., editors, Ultramafic Rocks and Eclogites in the Southern Appalachian Orogen: Petrology and Tectonic Significance: Southeastern Geology, v. 40, n. 3, p. 213–229.

Ownby, S. E., Miller, C. F., Berquist, P. J., Carrigan, C. W., Wooden, J. L., and Fullagar, P. D., 2003, U-Pb geochronology and geochemistry of a portion of the Mars Hill Terrane, North Carolina–Tennessee: Constraints on origin, history, and tectonic assembly, *in* Tollo, R. P., Corriveau, L., McLelland, J. B., and Bartholomew, M. J., editors., Proterozoic Tectonic Evolution of the Grenville Orogen in North America: Geological Society of America Memoir 197, p. 609–632, http://dx.doi.org/10.1130/0-8137-1197-5.609

Patchett, P. J., and Ruiz, J., 1989, Nd-isotopes and the origin of Grenville-aged rocks in Texas: Implications for Proterozoic evolution of the United States mid-continent region: Journal of Geology, v. 97, n. 6, p. 685–695, http://dx.doi.org/10.1086/629352

Patchett, P. J., Ross, G. M., and Gleason, J. D., 1999, Continental drainage in North America during the Phanerozoic from Nd isotopes: Science, v. 283, n. 5402, p. 671–673, http://dx.doi.org/10.1126/science.283.5402.671

Pavlides, L., 1981, The central Virginia volcanic-plutonic belt: an island arc of Cambrian(?) age: United States Geological Survey Professional Paper 1231-A, 34 p.

Pavlides, L., Gair, J. E., and Cranford, S. L., 1982, Central Virginia volcanic-plutonic belt as a host for massive sulfide deposits: Economic Geology, v. 77, n. 2, p. 233–272, http://dx.doi.org/10.2113/gsecongeo.77.2.233

Peters, B. J., and Owens, B. E., 2011, Mineralogical and geochemical constraints on the origin of ferruginous quartzites in the Chopawamsic Terrane, Piedmont Province, Virginia: Geological Society of America Abstracts with Program, v. 43, n. 2, p. 29.

Pettingill, H. S., Sinha, A. K., and Tatsumoto, M., 1984, Age and origin of anorthosites, charnockites, and granulites in the central Virginia Blue Ridge: Nd and Sr isotopic evidence: Contributions to Mineralogy and Petrology, v. 85, n. 3, p. 279–291, http://dx.doi.org/10.1007/BF00378106

Rogers, W. B., 1884, A reprint of annual reports and other papers on the geology of the Virginias: New York, D. Appleton and Co., 832 p.

Samson, S. D., Hibbard, J. P., and Wortman, G. L., 1995, Nd isotopic evidence for juvenile crust in the Carolina terrane, southern Appalachians: Contributions to Mineralogy and Petrology, v. 121, n. 2, p. 171–184, http://dx.doi.org/10.1007/s004100050097

Sawyer, E. W., 1986, The influence of source rock type, chemical weathering and sorting on the geochemistry of clastic sediments from the Quetico metasedimentary belt, Superior Province, Canada: Chemical Geology, v. 55, n. 1–2, p. 77–95, http://dx.doi.org/10.1016/0009-2541(86)90129-4

Smith, D. R., Barnes, C., Shannon, W., Roback, R., and James, E., 1997, Petrogenesis of Mid-Proterozoic granitic magmas: examples from central and west Texas: Precambrian Research, v. 85, n. 1–2, p. 53–79, http://dx.doi.org/10.1016/S0301-9268(97)00032-6

Spears, D. B., Owens, B. E., and Bailey, C. M., 2004, The Goochland-Chopawamsic Terrane Boundary, central Virginia Piedmont: U.S. Geological Survey Circular, Report C 1264, p. 223–245.

Stose, G. W., and Stose, A. I. J., 1948, Stratigraphy of the Arvonia slate, Virginia: American Journal of Science, v. 246, p. 394–412, http://dx.doi.org/10.2475/ajs.246.7.394

Taylor, S. R., and McLennan, S. M., 1985, The Continental Crust: Its Composition and Evolution: Oxford, Blackwell Scientific Publications, 312 p.

Tillman, C. G., 1970, Metamorphosed trilobites from Arvonia, Virginia: Geological Society of America Bulletin, v. 81, p. 1189–1200, http://dx.doi.org/10.1130/0016-7606(1970)81[1189:MTFAV]2.0.CO;2

Virginia Division of Mineral Resources, 1993, Geologic Map of Virginia: Virginia Division of Mineral Resources, scale 1:500,000.

Watson, T. L., and Powell, S. L., 1911, Fossil evidence of the age of the Virginia Piedmont slates: American Journal of Science, v. 31, p. 33–44, http://dx.doi.org/10.2475/ajs.s4-31.181.33

Wilson, J. R., ms, 2001, U/Pb ages of plutons from the Central Appalachians and GIS-based assessment of plutons with comments on their regional significance: Blacksburg, Virginia, Virginia Tech, M.S. thesis, 109 p.